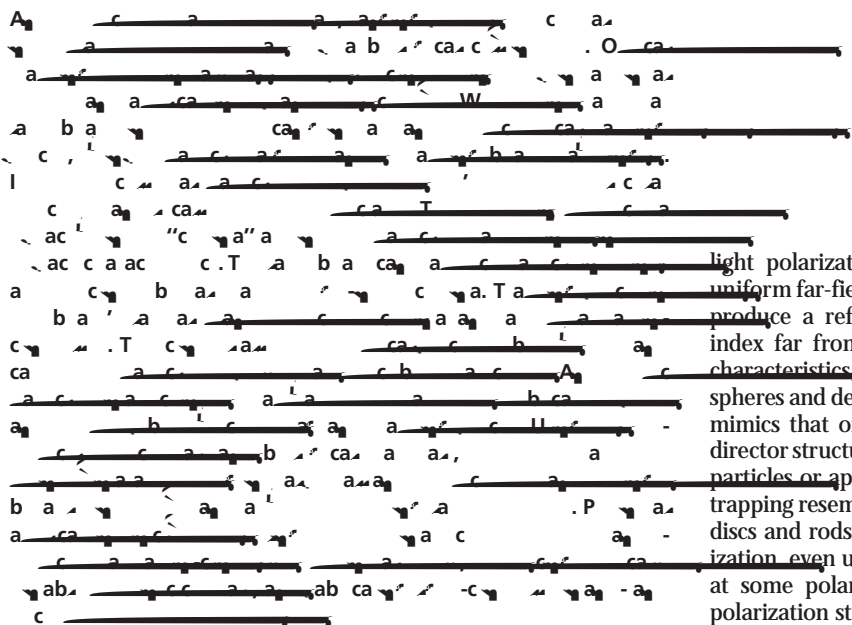


# Laser trapping in anisotropic fluids and polarization-controlled particle dynamics

I. S. Aronson<sup>a</sup>, V. Kacmar<sup>b</sup>, N. K. Pappa<sup>a</sup>, N. P. Aronson<sup>a</sup>

<sup>a</sup>Department of Physics, University of California, San Diego, La Jolla, California 92092, USA  
<sup>b</sup>Department of Physics, University of California, San Diego, La Jolla, California 92092, USA

Received 12 October 2006; revised 12 October 2006; accepted 12 October 2006



allow for measurement of colloidal forces (2, 23) mediated by LC elasticity (12, 19). Therefore, fundamental study of laser trapping properties in anisotropic fluids is of great significance.

In this article, we demonstrate that optical trapping of colloidal spheres in anisotropic fluids is direction sensitive and can be controlled by changing polarization of the beam. The unique trapping properties arise because of the following factors. A linearly polarized beam propagating in the anisotropic fluid "sees" the local effective refractive index  $n_{\text{eff}}$

that depends on the director  $\hat{N}$  and the light polarization state. A spherical particle in the LC with a uniform far-field director  $\hat{N}_0$  causes local director distortions, which produce a refractive index "corona" (RIC), different from  $n_{\text{eff}}$  index far from the sphere. By controlling the particle's surface characteristics, we generate well defined structures around the spheres and demonstrate that the angular pattern of trapping forces mimics that of the RIC. Trapping of the beads depends on the director structure, which can be changed by surface treatment of the particles or applying an external field (24). The direction-sensitive trapping resembles that of objects with an anisotropic shape such as discs and rods. Optical forces are varied by changing beam polarization even up to an extreme situation when a particle is trapped at some polarizations, but repelled from the beam with other polarization states. Control of particle dynamics by polarization of a stationary trap has potential optomechanic and photonic applications.

Fig. 1 shows optical polarizing microscopy (PM) images of particles with different RICs.

which is an optical axis of the common anisotropic fluids, the uniaxial liquid crystals (LCs). LCs are widely known for their applications in displays, telecommunications, and electro-optic devices (1). However, membranes, cytoskeleton proteins, amino acids, viruses, and lipids can form LC phases not only *in vitro* but even *in vivo* (2, 3). Self-organized structures of collagen in connective tissues (4) and in muscle fibers (4) and like actin and myosin organization in human spermatozoa (6, 7). Anisotropic suspensions (12, 13) and molecules (14) have attracted a great deal of attention because of their unique properties and potential applications. Anisotropic self-organization in a living cell's interior may play a vital biological function and is readily observed by means of interference imaging (15, 16). Recently, there has been a growing interest in optical trapping in anisotropic media (17–22). Laser tweezers can control dynamics of nano- and micro-objects and

Fig. 1 shows optical polarizing microscopy (PM) images of particles with different RICs. Fig. 1 A–D, light intensity  $I_{\text{PM}}$  is related to the local index  $n_{\text{eff}}$  averaged across the chamber thickness  $h$ , where  $\beta$  is the angle between the local director and a polarizer in PM. Experimental images are consistent with director structures (Fig. 1 E–L) that we obtain by using the *Ansatz* minimizing the Frank elastic free energy (12, 13, 25, 26) for respective boundary conditions at the particle's surface. We also calculate the patterns of  $n_{\text{eff}}$  for laser light linearly polarized perpendicular to the far-field director  $\hat{N}_0$  (Fig. 1 E–H) and parallel to it (Fig. 1 E–L). Clearly, the RICs around beads are polarization dependent (Fig. 1 E–L).

Surface treatment and confinement allow us to control the director  $\hat{N}$  and RIC (Fig. 1). The particles with tangential boundary conditions (Fig. 1 A) produce a quadrupolar pattern of  $\hat{N}$  and RIC (19). At the bead–LC interface,  $\hat{N}$  is parallel to the surface and continuously transforms to the far-field director  $\hat{N} \parallel \hat{N}_0$  far from the

bead (Fig. 1 *E* and *I*). The only defects are two surface point defects (called “boojums”) at the poles of a particle along  $\hat{N}_0$ . The colloidal beads that align  $\hat{N}$  perpendicular to their surfaces can produce dipolar (Fig. 1 *B*) or quadrupolar (Fig. 1 *C*) director structures and RICs; the structure type is controlled by the particle confinement into chambers of different thickness  $h$  (13). A dipole-type structure is formed in thick chambers of  $h \approx 30 \mu\text{m}$  much larger than the particle radius  $R \approx 1 \mu\text{m}$  (Fig. 1 *B*); the bead is accompanied by a point defect in  $\hat{N}$ , the hyperbolic hedgehog. A quadrupolar “Saturn-ring” configuration is observed in an  $h \approx 6 \mu\text{m}$  cell and contains a line defect (the disclination of a half-integer strength) encircling the particle in the equatorial plane perpendicular to  $\hat{N}_0$  (Fig. 1 *C*, *G*, and *K*). Finally, when surface anchoring forces are weak compared with bulk elastic forces, the uniform director structure is barely perturbed by the beads and  $\hat{N}$  strongly deviates from the tangential (Fig. 1 *D* and *L*) or perpendicular (Fig. 1 *H*) orientations at their surfaces.

All director structures in Fig. 1 have a rotational symmetry axis crossing the particle’s center parallel to the far-field director  $\hat{N}_0$ . The respective RICs have a mirror symmetry plane orthogonal to the substrates and crossing the particle’s center parallel to  $\hat{N}_0$ . In the case o (dev)-3paredan-15.73291.4(1)]15.736 1 Tf17.6147 056 T0 Tc(N)Tj0.1 1 Tf0.6381 0 TD58/

that would be mirror images of those shown in Fig. 2 *C* and *E*

the far-field director  $\hat{N}_0$  than perpendicular to it (Fig. 4 *A* and *B*), consistent with the theory (13, 27) and recent experiments (28). We determine diffusion coefficients  $D_{\parallel, \perp} = \frac{2}{\tau} \langle \delta \mathbf{N}_0 \cdot \delta \mathbf{N}_0 \rangle$  and find the ratio  $D_{\parallel} / D_{\perp} = 0.00573$  (theoretical)  $0.006226$  (TF6.5006105.6869g24.8) (theoretical)

shows that the studied anisotropic trapping properties are unique for anisotropic fluids.

**T B F**. In addition to thermotropic LCs, we also studied trapping in biological anisotropic fluids: aqueous solutions of  $\lambda$  phage DNA with optical anisotropy  $n = n_e - n_o = 0$  and FD virus with  $n = 0$ . In both cases,  $|n| = 0.01$  is small and the average LC index  $\bar{n}_{LC} = [(2n_o^2 + n_e^2)/3]^{1/2}$  is close to that of water  $n_w = 1.33$ . The anisotropy of trapping forces  $F_t$  in these systems is observed (10%) when trapping silica beads with  $n_p = 1.45$ . However, optical trapping is strong but direction insensitive for MR particles with  $n_p = 1.69$ . Moreover,  $F_t$

(19, 21). This behavior is in contrast to that in isotropic fluids, where calibration for only one direction in the lateral plane is sufficient (2). Moreover, Fig. 5B demonstrates that quantitative studies can be performed only for relatively low power. The measurements are easier in materials with low  $n$  for which the